Non-perturbative statistical theory of intermittency in ITG drift wave turbulence with zonal flows

Johan Anderson[1] and Eun-jin Kim
University of Sheffield
Department of Applied Mathematics
Hicks Building, Hounsfield Road
Sheffield
S3 7RH
UK

Abstract

The probability distribution functions (PDFs) of momentum flux and zonal flow formation in ion-temperature-gradient (ITG) turbulence are investigated, including the effect of the shear flow on the PDFs. While ITG turbulence maintains high level of transport, this may be suppressed by shear flow. Zonal flows are also shown here to have an enhanced likelihood of generation further from marginal stability which will then regulate the ITG turbulence, which is more prominent with increased shear flow, leading to a self-regulating system.

1 Introduction

One of the main challenges in magnetic fusion research has been to predict the turbulent heat and particle transport originating from various micro-instabilities. The ion-temperature-gradient (ITG) mode is one of the main candidates for causing the anomalous heat transport in core plasmas of tokamaks [1]. Significant heat transport can however be mediated by coherent structures such as streamers and blobs through the formation of avalanche like events of large amplitude, as indicated by recent numerical studies. These events cause the deviation of the probability distribution functions (PDFs) from a Gaussian profile on which the traditional mean field theory (such as transport coefficients) is based. A crucial question in plasma confinement is

[1]anderson.johan@gmail.com

thus the prediction of the PDFs of the transport due to these structures and of their formation.

The purpose of this research is to investigate the likelihood of the formation of coherent structures by computing the PDF (tails) of momentum flux and predict the PDFs of zonal flow formation [2]. An advanced fluid model for the ITG mode is used that has been successful in reproducing both experimental and non-linear gyro-kinetic results [3]. The theoretical technique used here is the so-called instanton method, a non-perturbative way of calculating the PDF tails. The PDF tail is first formally expressed in terms of a path integral by utilizing the Gaussian statistics (with delta correlation in time was chosen for the simplicity of the analysis) of an external forcing. An optimum path will then be associated with the creation of a modon (among all possible paths) and the action is evaluated using the saddle-point method on the effective action. The saddle-point solution of the dynamical variable $\phi(x,t)$ of the form $\phi(x,t) = F(t)\psi(x)$. The instanton is localized in time, existing during the formation of the modon. Thus, the bursty event can be associated with the creation of a modon. Note that, the function $\psi(x)$ here represents the spatial form of the coherent structure. The tails of PDF of global momentum flux and heat flux are shown to be stretched exponential with the form [4]- [8], which is broader than a Gaussian. This result suggests that rare events of large amplitude due to coherent structure are crucial in transport, offering a novel explanation for exponential PDF tails of momentum flux found in recent experiments at CSDX at USCD [9].

2 Non-perturbative calculation of structure formation PDF

The ITG mode turbulence is modeled using the continuity and temperature equation for the ions and considering the electrons to be Boltzmann distributed [3]. The effects of parallel ion motion, magnetic shear, trapped particles and finite beta on the ITG modes are neglected since in previous works the effect of parallel ion motion on the ITG mode was shown to be rather weak. The effect of a shear flow is incorporated in the time evolution equations for the background fluctuations in the form of sheared velocity V_0. The continuity and temperature equations then become,

$$\frac{\partial n}{\partial t} - \left(\frac{\partial}{\partial t} - \alpha_i \frac{\partial}{\partial y}\right)\nabla_\perp^2 \phi + \frac{\partial \phi}{\partial y} + V_0 \frac{\partial}{\partial y}\left(1 - \nabla_\perp^2\right)\phi -$$

$$\epsilon_n g_i \frac{\partial}{\partial y}\left(\phi + \tau\left(n + T_i\right)\right) + \nu\nabla^4\phi = -\left[\phi, n\right] + \left[\phi, \nabla_\perp^2 \phi\right] + \tau\left[\phi, \nabla_\perp^2\left(n + T_i\right)\right] + f \quad (1)$$

$$(\frac{\partial}{\partial t} + V_0\frac{\partial}{\partial y})T_i - \frac{5}{3}\tau\epsilon_n g_i \frac{\partial T_i}{\partial y} + \left(\eta_i - \frac{2}{3}\right)\frac{\partial \phi}{\partial y} - \frac{2}{3}(\frac{\partial}{\partial t} + V_0\frac{\partial}{\partial y})n =$$

$$- [\phi, T_i] + \frac{2}{3} [\phi, n] . \quad (2)$$

Eqs. (1)-(2) are closed by using the quasi-neutrality condition. Here $[A, B] = (\partial A/\partial x)(\partial B/\partial y) - (\partial A/\partial y)(\partial B/\partial x)$ is the Poisson bracket; f is a forcing; $n = (L_n/\rho_s)\delta n/n_0$, $\phi = (L_n/\rho_s)e\delta\phi/T_e$, $T_i = (L_n/\rho_s)\delta T_i/T_{i0}$ are the normalized ion particle density, the electrostatic potential and the ion temperature, respectively. In equations (1) and (2), $\tau = T_i/T_e$, $\rho_s = c_s/\Omega_{ci}$ where $c_s = \sqrt{T_e/m_i}$, $\Omega_{ci} = eB/m_i c$ and ν is collisionality. We also define $L_f = -\left(dlnf/dr\right)^{-1}$ $(f = \{n, T_i\})$, $\eta_i = L_n/L_{T_i}$, $\epsilon_n = 2L_n/\bar{R}$ where $\bar{R}$ is the major radius and $\alpha_i = \tau\left(1 + \eta_i\right)$. The perpendicular length scale and time are normalized by ρ_s and L_n/c_s, respectively. The geometrical quantities are calculated in the strong ballooning limit ($\theta = 0$, $g_i\left(\theta = 0\right) = 1$, with $\omega_\star = k_y v_\star = \rho_s c_s k_y/L_n$). It should be noted that the time evolution of the zonal flow potential (ϕ_{ZF}) is governed by an averaged Eq. (1) [see last line in Eq. (6)]. This is equivalent to using the electron density response $n_e = \phi - \langle\phi\rangle$ [10].

We calculate the PDF tails of momentum flux and zonal flow formation by using the instanton method. To this end, the PDF tail is expressed in terms of a path integral by utilizing the Gaussian statistics of the forcing f. The probability distribution function of Reynolds stress $Z_1 = R$ and zonal flow formation $Z_2 = \phi_{ZF}$ (using the notation Z_j for j=$\{1,2\}$) can be defined as

$$\begin{aligned} P(Z) &= \langle\delta(Z_j - Z)\rangle \\ &= \int d\lambda_j \exp(i\lambda_j Z)\langle\exp(-i\lambda_j Z_j)\rangle \\ &= \int d\lambda_j \exp(i\lambda_j Z) I_{\lambda_j}, \end{aligned} \quad (3)$$

where

$$I_{\lambda_j} = \langle\exp(-i\lambda_j Z_j)\rangle. \quad (4)$$

The integrand can then be rewritten in the form of a path-integral as

$$I_{\lambda_j} = \int \mathcal{D}\phi\mathcal{D}\bar{\phi}\mathcal{D}\phi_{ZF}\mathcal{D}\bar{\phi}_{ZF} e^{-S_{\lambda_j}}. \quad (5)$$

Here, the parameter j refers to the two specific cases included in the present study; namely $j = 1$ gives the PDF tail of momentum flux while $j = 2$ the PDF tail of the structure formation. The angular brackets denote the average over the statistics of the forcing f. By using the ansatz $T_i = \chi\phi$, the effective action S_{λ_j} in Eq. (5) can be expressed as,

$$S_{\lambda_j} = -i \int d^2x dt \bar{\phi} \left(\frac{\partial\phi}{\partial t} - (\frac{\partial}{\partial t} - \alpha_i \frac{\partial}{\partial y})\nabla_\perp^2\phi + V_0(1 - \nabla_\perp^2)\phi \right.$$

$$
\begin{aligned}
&+ \quad (1-\epsilon_n g_i\beta)\frac{\partial\phi}{\partial y} - \beta[\phi,\nabla_\perp^2\phi]\Big) \\
&+ \quad \frac{1}{2}\int d^2x d^2x' \bar{\phi}(x)\kappa(x-x')\bar{\phi}(x') \\
&+ \quad i\lambda_1\int d^2x dt(-\frac{\partial\phi}{\partial x}\frac{\partial\phi}{\partial y})\delta(t) \\
&+ \quad i\lambda_2\int dt\phi_{ZF}(t)\delta(t) \\
&- \quad i\int dt\bar{\phi}_{ZF}(t)(\frac{\partial\phi_{ZF}(t)}{\partial t} + \langle v_x v_y\rangle). \qquad (6)
\end{aligned}
$$

Note that the PDF tails of momentum flux and structure formation can be found by calculating the value of S_{λ_j} at the saddle-point in the two cases $\lambda_1 \to \infty, \lambda_2 = 0$ or $\lambda_1 = 0, \lambda_2 \to \infty$, respectively. Here the term $\langle v_x v_y\rangle$ is the Reynolds stress averaged over the forcing (f) and space. that generates the zonal flow. The first case $\lambda_1 \to \infty, \lambda_2 = 0$ gives the PDF tail of momentum flux in ITG turbulence including the interaction of a shear flow (V_0) while the second limit $\lambda_1 = 0, \lambda_2 \to \infty$ gives the PDF tail of zonal flow formation. In Eq. (6) we have used,

$$
\begin{aligned}
\beta &= 1+\tau+\tau\chi, \qquad (7) \\
\chi &= \frac{\eta_i - \frac{2}{3}(1-U+V_0)}{U-V_0+\frac{5}{3}\tau\epsilon_n g_i}. \qquad (8)
\end{aligned}
$$

In Eq. (8), U is the modon speed. To obtain Eq. (6) we have assumed the statistics of the forcing f to be Gaussian with a short correlation time modeled by the delta function as

$$
\langle f(x,t)f(x',t')\rangle = \delta(t-t')\kappa(x-x'), \qquad (9)
$$

and $\langle f\rangle = 0$. The delta correlation in time was chosen for the simplicity of the analysis. In the case of a finite correlation time the non-local integral equations in time are needed.

3 The PDF tails

The PDF tails are found by calculating the value of S_{λ_j} using Eq. (6) at the saddle-point in the two cases; the PDF tail of momentum flux by taking into account the effect of a shear flow ($\lambda_1 \to \infty, \lambda_2 = 0$) and the PDF tail of structure formation of zonal flow ($\lambda_1 = 0, \lambda_2 \to \infty$). The integral in Eq (6) is divided in four parts C_1 the ITG integral; C_2 the forcing integral; C_3 the momentum flux integral; C_4 the zonal flow integral and finally C_5 represents the zonal flow evolution integral. The resulting integrals in the first case are;

$$
S_{\lambda_1} \simeq -\frac{1}{3}ih\lambda_1^3, \qquad (10)
$$

$$h = C_1 + C_2 + C_3 + C_4 + C_5, \tag{11}$$

$$C_1 = \frac{1}{2\kappa_0}\left(\gamma^2(1+\epsilon^2)[(\frac{4H_0}{H_0-1}-1)^{3/2}-1]\frac{C^{3/2}}{A}\right. \tag{12}$$

$$\left. + \; 24(1+6\epsilon^2)\gamma_2^2\frac{C^{3/2}}{A^{5/2}}(\frac{1}{3}\frac{H_0}{(H_0-1)^3}-\frac{1}{4}\frac{H_0}{(H_0-1)^2})\right), \tag{13}$$

$$C_2 = \frac{1}{2\kappa_0}\left(\gamma^2(1+\epsilon^2)[(\frac{4H_0}{H_0-1}-1)^{3/2}-1]\frac{C^{3/2}}{2A}\right. \tag{14}$$

$$\left. + \; 24(\frac{1}{2}+2\epsilon^2)\gamma_2^2\frac{C^{3/2}}{A^{5/2}}(\frac{1}{3}\frac{H_0}{(H_0-1)^3}-\frac{1}{4}\frac{H_0}{(H_0-1)^2})\right), \tag{15}$$

$$C_3 = R_0F^2(0),\; C_4 = 0, \tag{16}$$

$$C_5 = \frac{2R_0\sqrt{C}}{A}\frac{1}{H_0-1}, \tag{17}$$

$$H_0 = 4A-2,\; A = \frac{\eta}{(1+\epsilon^2)\gamma^2}. \tag{18}$$

Here $C = 2\kappa_0\lambda_1^2/((1+\epsilon^2)\gamma)$ or $C = 2\kappa_0\lambda_2/((1+\epsilon^2)\gamma)$, $\gamma = c_1(1+k^2+2\alpha/k^3)$ (k is the modon wave number), $c_1 = \alpha a/J_1(ka)$ (a is the modon size), $\alpha = A_1 - k^2A_2$, $A_1 = (1-\epsilon_n - U + V_0)/\beta$, $A_2 = (\alpha_i + U - V_0)/\beta$, $\gamma_2 = k\beta\alpha/2$, $\eta = (1+6\epsilon^2)\gamma_2^2$ and κ_0 is the strength of the forcing $\kappa(x-y)$. To obtain the integrals in Eq. (6) we have used the localized modon solution, involving the parameter ϵ. The PDF tail of the Reynolds stress (R) can now be found by performing the integration over λ_1 in Eq. (6) using the saddle-point method in the same fashion as done in Ref. [7]- [8] i.e. recall Eq. (3) gives $P(R) \sim \int d\lambda_1 \exp\{-i\lambda_1 R - S_{\lambda_1}\} \sim \int d\lambda_1 \exp\{-i\lambda_1 R + ih\lambda_1^3\}$. Now, the saddle point integral is evaluated at the saddle point $\lambda_{1MAX} = \sqrt{R/(3h)}$ which maximizes $P(R)$ with the result

$$P(R) \sim \exp\{-\xi_1(\frac{R}{R_0})^{3/2}\}, \tag{19}$$

$$\xi_1 = \frac{2}{3}\frac{1}{\sqrt{3h}}. \tag{20}$$

This result is similar to the previous ones where a similar exponential PDF was found. However, here the coefficient ξ_1 is different due to the presence of the shear flow (V_0).

In the second limit where $\lambda_1 = 0$ and $\lambda_2 \to \infty$ gives the PDF tail of the structure formation itself, the action integral yields

$$S_{\lambda_2} \simeq -ih\lambda_2^{3/2}, \tag{21}$$

$$C_3 = 0,\; C_4 = 2\phi_{ZF0}\frac{\sqrt{C}}{A}. \tag{22}$$

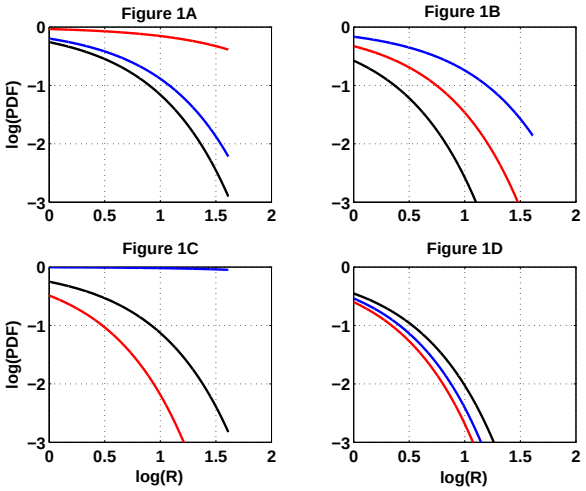

Figure 1: (Color online). The PDF tail of momentum flux in ITG turbulence incorporating the effects of shear flow for $V_0 = 0.0$ (Figure 1A), $V_0 = 5.0$ (Figure 1B), $V_0 = 10.0$ (Figure 1C) and $V_0 = 15.0$ (Figure 1D) for $\eta_i = 2.0$ (red), $\eta_i = 4.0$ (blue) and $\eta_i = 6.0$ (black).

The PDF tail can now be computed in a similar way as done previously with the result

$$P(\phi_{ZF}) \sim \exp\{-\xi_2(\phi_{ZF}/\phi_{ZF0})^3\}, \tag{23}$$

$$\xi_2 = \frac{4}{27}\frac{1}{h^2}. \tag{24}$$

Recall that in the computation of the PDF tails of the zonal flow structure formation, the zonal flow was assumed to be driven by a modon in the ITG turbulence since the bipolar vortex soliton (modon) was assumed to be created by the forcing and that $F(t) = 0$ as $t \to -\infty$. Thus we could view Eqs (20) and (24) as the transition amplitudes from an initial state with no fluid motion to a state with with different R/R_0 or ϕ_{ZF}/ϕ_{ZF0}.

4 Results and discussion

We have presented a theory of the PDF tail of structure formation and how the PDF tail of momentum flux is modified by the presence of a shear flow. The exponential forms of the two PDF tails are completely different, signifying the difference in the physical interpretation. In the case of structure formation the PDF tails are found as $\sim \exp\{-\xi_2\phi_{ZF}^3\}$, while the momentum flux PDF tail $\sim \exp\{-\xi_1 R^{3/2}\}$. The origin of these scalings are the quadratic non-linearity in the dynamical system (Eqs 1-2). The difference in scaling of the PDF tails momentum flux and zonal formation comes from the change

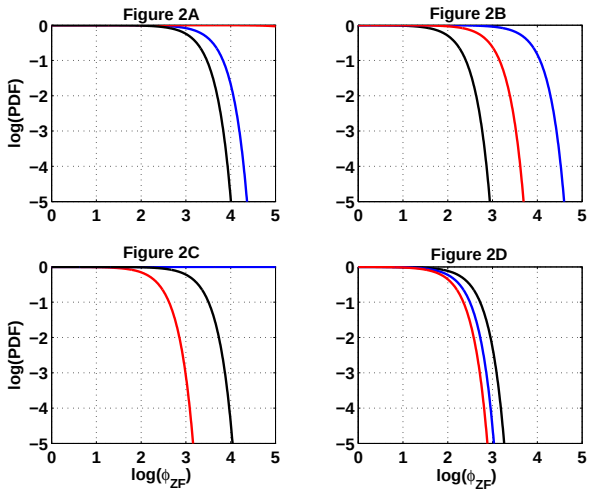

Figure 2: (Color online). The PDF tail of zonal flow formation in ITG turbulence incorporating the effects of shear flow for $V_0 = 0.0$ (Figure 2A), $V_0 = 5.0$ (Figure 2B), $V_0 = 10.0$ (Figure 2C) and $V_0 = 15.0$ (Figure 2D) for $\eta_i = 2.0$ (red), $\eta_i = 4.0$ (blue) and $\eta_i = 6.0$ (black).

in the temporal behavior of the modon (a change in the initial condition F_0). The spatial structure of the modon is of less importance in determining the exponent in the exponential PDF tails than the temporal behavior, but changes the overall amplitude through the coefficients ξ_1 and ξ_2. Therefore an approximate spatial structure is sufficient to determine the exponential scaling whereas the time dependency may affect the scaling. The spatial structure of the flow is incorporated in the initial condition of the flow ϕ_{ZF0}. In this section the parametric dependencies of ξ_j will be studied in detail. First the PDF tail of momentum flux in ITG turbulence incorporating the effects of shear flow is shown in Figure 1. The parameters are $\tau = 0.5$, $\epsilon_n = 1.0$, $g_i = 1$, $a = 2$, $U = 2.0$, $\kappa_0 = 3000$, $\epsilon = 0.1$, $k \approx 1.91$ with $V_0 = 0.0$ (Figure 1A), $V_0 = 5.0$ (Figure 1B), $V_0 = 10.0$ (Figure 1C) and $V_0 = 15.0$ (Figure 1D) for $\eta_i = 2.0$ (red), $\eta_i = 4.0$ (blue) and $\eta_i = 6.0$ (black). When $V_0 = 0$, the result recovers the previous finding in Ref. [7]. It is clearly shown that the PDF tail of momentum flux is significantly reduced if a strong shear flow is present whereas weak flow can increase the PDF tail. In the equations the flow speed and the modon velocity comes in as a combination of the form $(U - V_0)$, determining the behavior of the resulting PDF tails. When $(U - V_0)$ decreases, the PDF tail increases until it eventually decreases. This means that there exists a negative value $(U - V_0)$ that gives maximum PDF tail, depending on all other parameters. Note that although the Galilean invariance of Eq. (1)-(2) may allow us to perform Galilean transformations to find other instanton solutions, those solutions correspond to different ground states in the field theory and must be discarded since they have nonzero velocity in the

infinite past [11]. Thus, our instanton solutions are not Galilean invariant.

Second, the PDF tails of structure formation in ITG turbulence incorporating the effects of shear flow is shown in Figure 2. The parameters and the interpretation of the results are the same as those in Figure 1.

In summary, this paper presents the first prediction of the PDF tails of zonal flow formation. One of the important results is that shear flows can significantly reduce the PDF tails of momentum flux and zonal flow formation. Since zonal flows are more likely to be generated further from marginal stability, they will then regulate ITG turbulence, leading to a self-regulating system. Namely, while ITG turbulence is a state with high level of heat flux, it also generates stronger zonal flows that inhibit transport.

5 Acknowledgment

This research was supported by the Engineering and Physical Sciences Research Council (EPSRC) EP/D064317/1.

References

[1] W. Horton, Rev. Mod. Phys. **71**, 735 (1999)

[2] P. H. Diamond, S-I. Itoh, K. Itoh and T. S. Hahm, Plasma Phys. Contr. Fusion **47** R35 (2005)

[3] J. Anderson, H. Nordman, R. Singh and J. Weiland, Phys. Plasmas **9**, 4500 (2002)

[4] E. Kim and P. H. Diamond, Phys. Plasmas **9**, 71 (2002)

[5] E. Kim and P. H. Diamond, Phys. Rev. Lett. **88**, 225002 (2002)

[6] E. Kim, P. H. Diamond, M. Malkov, T.S. Hahm, *et al* , Nucl. Fusion **43**, 961 (2003)

[7] J. Anderson and E. Kim, Phys. Plasmas, **15** 052306 (2008)

[8] J. Anderson and E. Kim, Phys. Plasmas, in press (2008)

[9] Z. Yan et al, 49th APS-DPP November 12-16, Orlando, Florida, USA (2007)

[10] F. Jenko, W. Dorland, M. Kotschenreuther and B. N. Rogers, Phys. Plasmas **7**, 1904 (2000)

[11] V. Gurarie and A. Migdal, Phys. Rev. E **54**, 4908 (1996)